Colloid Polym Sci (2004) 282: 918–926
DOI 10.1007/s00396-004-1127-y

ORIGINAL CONTRIBUTION

Florian Nettesheim
Claus B. Müller
Ulf Olsson
Walter Richtering

Shear-induced sponge-to-lamellar phase transition studied by rheo-birefringence

Received: 20 February 2004
Accepted: 1 April 2004
Published online: 1 May 2004

F. Nettesheim · C. B. Müller
Physical Chemistry,
Christian-Albrechts-Universität zu Kiel,
Olshausen Str. 40, 24098 Kiel, Germany

U. Olsson
Physical Chemistry 1,
Lund University, Getingevägen 60,
Box 124, 221 00 Lund, Sweden

W. Richtering (✉)
Physical Chemistry, RWTH-Aachen,
Templergraben 59,
52056 Aachen, Germany
E-mail: richtering@rwth-aachen.de

Abstract We report on the shear induced transition from the L_3- to the L_α-phase studied by means of flow birefringence using the system pentaethyleneglycol monododecylether ($C_{12}E_5$), decane, water. The dependence of the critical shear rate, at which the transition from the isotropic state to the anisotropic takes place, on membrane volume fraction was studied in temperature ramp experiments at different constant shear rates and in isothermal shear ramp experiments. These results are compared with relaxation experiments from the shear aligned state back to the isotropic. For all these experiments power law exponents in the membrane volume fraction between 1.6 and 2.8 were found, which are rather low compared to values of current theories. The values found for the inverse critical shear rate and the decay times from the relaxation experiments differ by four orders of magnitude.

Introduction

Lyotropic surfactant systems display a rich phase behavior. Phase diagrams of nonionic surfactants, for instance of the C_nE_m-type, where n is the number of carbons in the hydrocarbon chain and m the number of ethylene oxide units in the headgroup of the surfactant, display a large temperature and concentration range, with micellar aggregates organized as bilayers. These themselves can arrange in stacks (L_α-phase) or divide the sample volume into two bicontinuous interpenetrating subvolumes (L_3- or sponge phase).

Of particular interest is the behavior of these phases under shear, because detailed knowledge of the influence of shear is relevant for industrial applications [1, 2]. The L_3-phase itself is known to be flow birefringent and small-angle neutron scattering (SANS) experiments revealed that a transition from the sponge-phase to a shear aligned lamellar phase takes place above a critical shear rate $\dot{\gamma}_c$, that depends strongly on membrane volume fraction [3]. Such a transition from an isotropic to the L_α-phase was discussed theoretically by Cates and Milner [4]. They found the following relationship between the critical shear rate and membrane volume fraction Φ_m:

$$\dot{\gamma}_c \propto \frac{k_b T}{\eta_s \xi^3} \propto \frac{k_b T}{\eta_s} \left(\frac{\Phi_m}{\delta}\right)^3 \quad (1)$$

where k_b is Boltzmann's constant, ξ the correlation length of the L_3-phase, η_s the solvent viscosity, and δ the thickness of the bilayer. They also predicted that the

critical temperature (L_3 to $L_3 + L_\alpha$) and spinodal should have different shear rate dependencies leading to an increasingly narrow two-phase region and consequently to weakening of the first order character of the transition.

Different behavior of the L_3-phase under shear was predicted by Bruinsma and Rabin [5]. Based on the Reynolds effect, enhancement of concentration fluctuations is found, which stabilizes the L_3- over the L_α-phase.

More recently, Porte et al. [6, 7, 8] studied the shear induced isotropic-to-nematic transition in wormlike micellar systems in rate-controlled experiments and concluded that it has all the characteristics of a first-order phase transition. The transition involves shear bands in the two-phase region accompanied by a stress plateau. Within the framework of a first-order transition it was possible to scale the rheological data of different concentrations and temperatures on to a master curve using reduced variables $\dot{\gamma}^* = \dot{\gamma}\tau_r$ and $\sigma^* = \sigma/G_0$. Here τ_r is the terminal relaxation time of a Maxwell fluid and G_0 its plateau modulus. Such behavior can also be assumed for the L_3-phase, although there are fundamental differences between the L_3-phase and wormlike micellar systems; for instance the L_3-phase, in contrast with wormy micelles (above the overlap concentration c^*), is not viscoelastic [9].

To investigate the underlying mechanisms more closely, a variety of L_3-phase systems was studied on length scales of the order of ξ, commonly using SANS and SAXS [3, 10, 11, 12, 13, 14, 15, 16]. Larger length scales were studied by dynamic light scattering (DLS), whereby the collective diffusion can be measured [3, 17, 18]. Temperature jump (T-jump) experiments were conducted by Le et al. [17, 18] and Schwarz et al. [19] to study the relaxation from a disturbed state back to equilibrium. All these studies aimed at correlating the dynamics of the system, i.e. membrane strangling, passage fission, and membrane fusion, to the observed transition under shear.

A systematic study in this respect was performed by Porcar et al. who used rheo-small-angle neutron scattering to investigate the structural changes in situ. Moreover, they used different membrane volume fractions and controlled the dynamics of the system by adding sugar to the L_3-phase. Thus the solvent viscosity of the "sweetened" sponge phase, which also enters Eq. (1), was varied over more than a decade. They found a scaling of the normalized sample viscosities (η/η_0 where η_0 is the solvent viscosity) and the anisotropy parameters from radial and tangential beam SANS experiments with $\dot{\gamma}\eta_s/\Phi_m{}^3$, in very good agreement with the predictions from theory [13].

Different experiments, however, probe different relaxation processes, and therefore different Φ_m-dependences are found in the literature. Le et al. for instance found that the relaxation of a perturbation by temperature-jump in case of the $C_{12}E_5$/decane/water system displayed a very strong Φ_m-dependence (if fitted to a powerlaw an exponent of -11 resulted) [17, 18]. They concluded that the relaxation is dominated by topology changes. However, this strong concentration dependence of the topological relaxation at low Φ_m can only be explained by a very high activation barrier of $350k_bT$ attributed to the formation of passages by membrane fusion. This high activation barrier, however, is in disagreement with current theories [4, 20].

Yamamoto et al. [21] studied the shear rate dependence of the transition temperature to the shear aligned L_α-phase of a dilute $C_{12}E_5$/water sample ($c = 1.8$ wt%) using small-angle light-scattering under shear and found reasonable agreement with the respective predictions of Cates and Milner.

A flow-birefringence study was performed by Mahjoub et al. [10], who raised the question of the role of defects in the shear-induced transition for the L_3-to-lamellar transition. They also found a weaker Φ_m-dependence than Porcar et al., raising the question whether the viscosity in Eq. (1) is that of the sample and not the solvent.

Here, we present data from a study using $C_{12}E_5$, decane, and water at a fixed surfactant to oil ratio, varying the membrane volume fraction. The critical temperature and the transition to the aligned L_α-phase was recorded as a function of shear rate. To study the critical shear rate more closely isothermal shear ramps were performed. The relaxation kinetics were studied in shear quench experiments. The transitions from L_3 to $L_3 + L_\alpha$ to L_α were tracked using birefringence and transmission measurements under shear.

Experimental

The sample under study consisted of the nonionic surfactant pentaethylene mono-dodecyl-ether ($C_{12}E_5$), *n*-decane and water. The decane-to-surfactant weight ratio was kept constant at 0.481:0.519 and only the water content was changed. Thus membrane thickness remained constant at 5 nm [18], while membrane volume fraction Φ_m was varied between 0.0388 and 0.31. Samples were prepared by diluting a stock solution of decane and $C_{12}E_5$ with water and mixing overnight to ensure equilibration.

Flow-birefringence experiments were performed in a stress-controlled Bohlin CVO-R rheometer equipped with a transparent plate–plate shear geometry. Birefringence and transmission were recorded by a commercially available optical analysis module (OAM) purchased from Rheometrics, which is mounted on the optical bench such that the laser passes the sample along the velocity gradient direction. A sample thickness of 0.2 mm was chosen for all experiments.

In a first series of experiments, the temperature was gradually increased at different constant shear rates. The temperature gradient was d T/d $t = 10$ K h^{-1}. The L_3-phase was identified at rest and also at low shear rates as the isotropic state, i.e. its birefringence $\Delta n \approx 0$.

In a second set of experiments the influence of shear on the sponge phase was studied at constant temperature. For this purpose a shear ramp was applied to the sample at a temperature which was, at rest, slightly above the upper L_3-phase boundary.

Finally, shear quench experiments were conducted, tracing the birefringence and transmission signals, to study the relaxation from the shear-aligned state back to the isotropic state.

Because the stability of the L_3-phase is very delicate with respect to composition and temperature, reversibility experiments were performed. The transition temperatures were checked in a temperature-dependence experiment at a shear rate of 10 s^{-1} performing successive heating and cooling cycles using the same sample filling. One temperature ramp took about one hour. Water evaporation was suppressed by a solvent trap situated around the shear geometry covered with lids. The transition temperatures of the heating and cooling experiments were found to be very similar. Thus we assume that selective evaporation of one component did not play a significant role during one experiment, which never took longer than two hours. For the following experiments samples were always freshly refilled. The problem of temperature gradients within the sample is also not of importance, since the sample thickness was 0.2 mm in the plate–plate geometry.

Results

To localize the very narrow region of the L_3-phase the phase boundaries of the system at rest used in this study were examined beforehand in a temperature bath equipped with crossed polarizers in a temperature range from 25 to 50 °C. Figure 1 displays the phase diagram as it was obtained from the inspection in the temperature bath.

Figure 2 displays transmission and birefringence data in addition to transient viscosities for a sample with a membrane volume fraction of $\Phi_m = 0.155$ representative of the experimental procedure used in this study. The L_3-phase was identified as the isotropic region following the L_α-phase (which itself can be isotropic due to parallel (homeotropic) orientation of the lamellae). The critical shear rate is determined as the drop of birefringence and transmission upon increasing the shear rate. The plate–plate geometry used throughout the investigation implies that the shear field is inhomogeneous, i.e. the shear rate increases with radius toward the outside. Hence the viscosities are average values over the whole volume of the shear geometry. If a transition takes place at a given shear rate (and thus a given radius) the viscosities of that particular volume can be different from the rest of the sample.

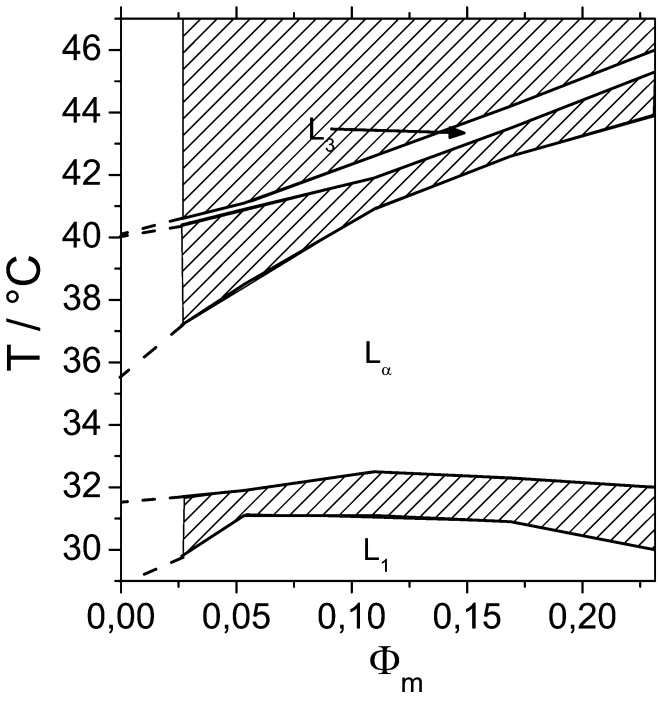

Fig. 1 Boundaries between L_1-, L_α-, and L_3-phases. *Hatched areas* indicate the two-phase regions

Nevertheless, the use of the plate–plate geometry has advantages. First, sample loss at high temperatures is much less pronounced than in a cone–plate geometry. Second, the cone–plate geometry bears the problem of viscoelastic meniscus distortions [22] at high shear rates, which can impede the birefringence experiments. Third, the sample thickness can be varied in a plate–plate geometry, which can be advantageous for the birefringence experiment. Finally, a shear-induced transition can be directly visualized as shown in Fig. 3. The nominal shear rate is determined at 3/4 of the radius of the shear geometry, the position at which also the laser for birefringence measurements passes the sample. Hence the birefringence corresponds to the shear rate selected in the control software.

In the following three sections we will present the results of the three different types of experiments performed in this study following the outline given in the experimental part.

Temperature-dependence experiments

In the temperature-scan experiments a constant shear rate was applied, while the sample was heated starting from the L_α-phase as found in the phase diagram at

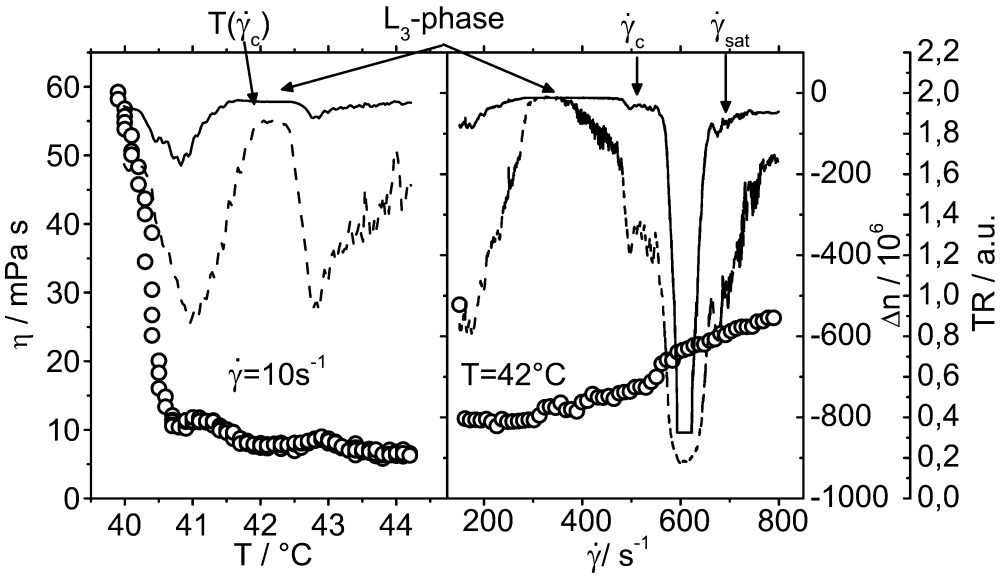

Fig. 2 Transmission (*dashed line*), birefringence (*solid line*), and transient viscosities (*open circles*) in a temperature ramp experiment (*left*) and an isothermal shear ramp (*right*) for $\Phi_m = 0.155$. $T(\dot{\gamma}_c)$, $\dot{\gamma}_c$, and $\dot{\gamma}_{sat}$ are the temperature of the transition $(L_3 + L_\alpha) \rightarrow L_3$ under shear, the critical shear rate (onset of birefringence), and the saturation shear rate, respectively

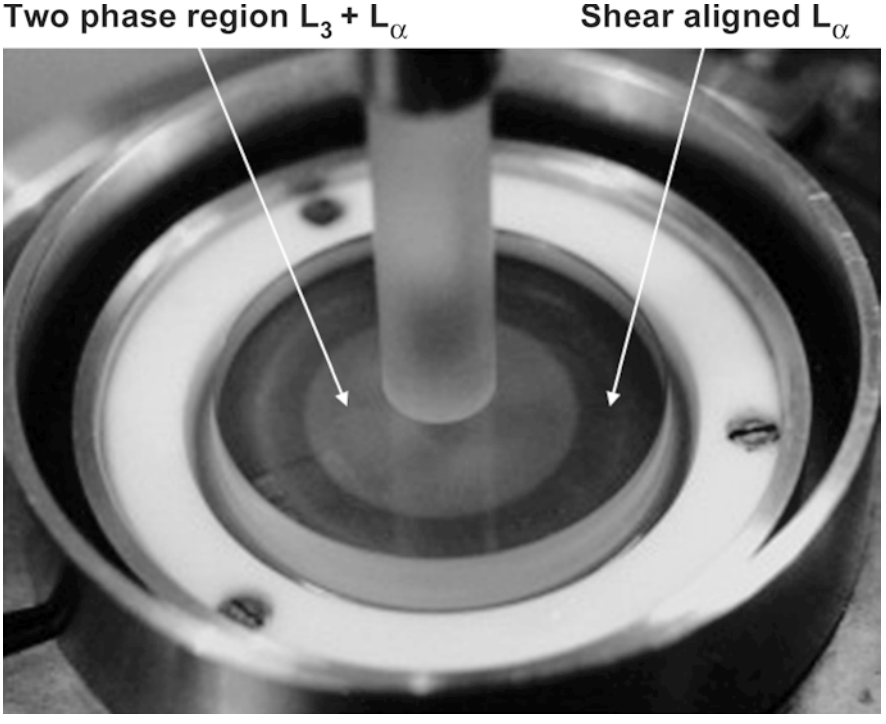

Fig. 3 L_3-phase under shear. Because of the inhomogeneous shear field in the plate–plate shear-geometry, the shear induced L_α-phase is visible at the outside, the two-phase region as a ring

rest. At low shear rates this was usually 39 °C. The results of these temperature-scan experiments are summarized in a phase diagram under shear for three different membrane volume fractions in Fig. 4. The lower and upper phase boundaries of the L_3-phase display a sudden shift to higher temperatures at a characteristic shear rate $\dot{\gamma}_c$. This shear rate shifts toward higher values as Φ_m increases. Also, the magnitude of the shift of the phase boundaries to higher temperature increases with concentration. Figure 5 displays the results of $\Phi_m = 0.0775$ along with the upper phase boundary of the L_α-phase, which seems to follow parallel to the lower L_3-phase boundary. The same behavior is found for the other samples. Thus there is always a two-phase region separating the L_3-phase from the shear induced L_α-phase, an indication of the first-order nature of the transition. The data, however, do not allow any conclusion of whether its first-order nature becomes weaker, as was predicted by Cates and Milner [4].

Isothermal experiments

The determination of the critical shear rate by the method used above suffers from the problem that it is not very accurate and these measurements thus only served as a means to map the phase region. The inaccuracy became most apparent when studying the lowest volume fraction $\Phi_m = 0.0388$. Owing to the low membrane volume fraction the signal in birefringence and the decrease in transmission were hardly detectable. Therefore, a correct determination of the critical shear rate was not possible in that case.

Isothermal measurements were performed with a wide range of volume fractions between $\Phi_m = 0.058$ and 0.31, where the shear rate was incrementally increased from 10 s^{-1} well into the shear-induced L_α-phase. For volume fraction $\Phi_m = 0.0388$ the lowest shear rate was chosen to be 4 s^{-1}, because from the preliminary experiments $\dot{\gamma}_c$ could be estimated to be ca. 10 s^{-1}.

In the isothermal experiments the critical shear rate was identified from the abrupt increase of the magnitude of birefringence accompanied by a decrease in transmission, thus with the transition from L_3 to the coexistence of L_3 and L_α (Fig. 2). These shear rates are very similar to $\dot{\gamma}_c$ from the temperature-scan experiments.

The critical shear rates determined for different volume fractions using this procedure are presented in Fig. 6. The critical shear rate displays a Φ_m–dependence with an exponent of 1.7. The transition to the pure shear-induced L_α-phase, however, displays Φ_m^2-dependence (Fig. 6). These exponents are not in good agreement with Eq. (1). On the other hand, deviations from the expected behavior have been reported previously by Mahjoub et al. [10], who also found an exponent smaller than 3. They argued that the viscosity in Eq. (1) is not that of the solvent but rather the sample viscosity, which itself can be Φ_m-dependent. Also, the exponent of approximately 2 found here for the critical shear rate happens to be similar to the scaling of the transition temperatures at rest [18].

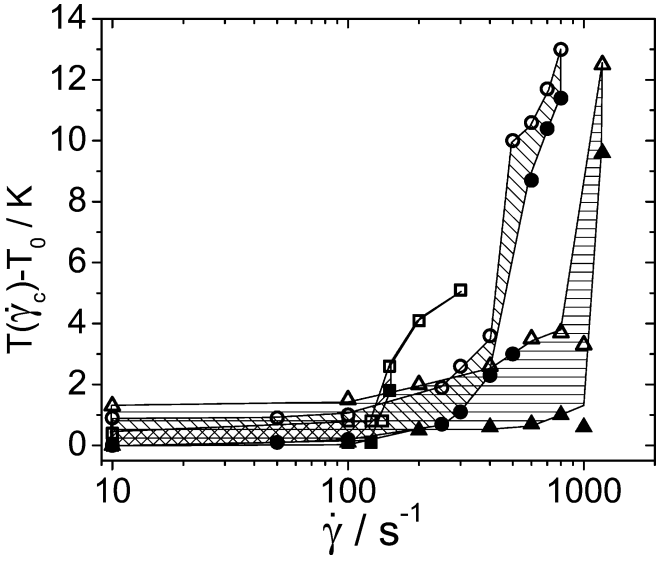

Fig. 4 Transition temperatures from $(L_\alpha + L_3)$ to L_3 to $(L_3 + H_2O)$ at different shear rates and three different membrane volume fractions $\Phi_m = 0.0775$ (*squares*), 0.155 (*circles*), and 0.2325 (*triangles*). *Closed* and *open* symbols depict the lower and upper L_3-phase boundaries, respectively

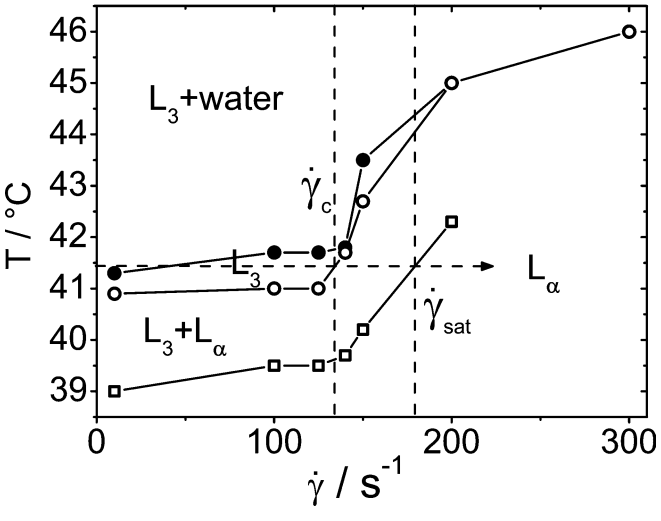

Fig. 5 Transition temperatures at different shear rates and $\Phi_m = 0.0775$. The *vertical lines* mark the critical ($\dot{\gamma}_c$) and saturation shear rate ($\dot{\gamma}_{sat}$), respectively. The *horizontal arrow* indicates how an isothermal shear ramp experiment was performed

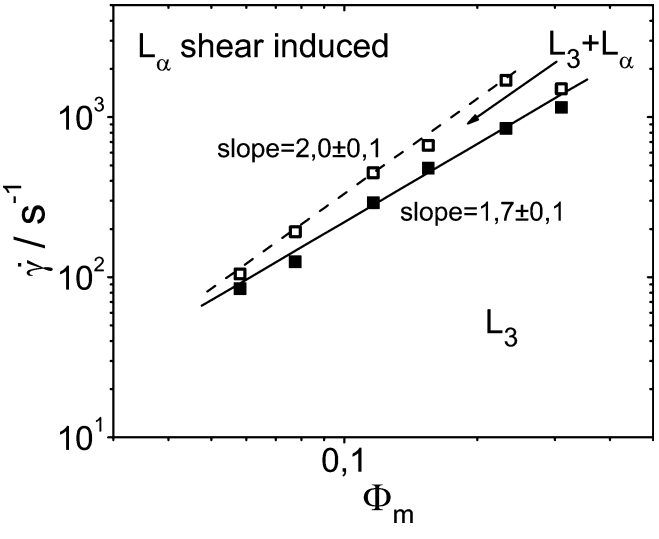

Fig. 6 Shear rates for the transition to the two-phase region (critical shear rate $\dot{\gamma}_c$, *solid squares*) and to the fully shear-aligned L_α-phase (saturation shear rate $\dot{\gamma}_{sat}$, *open squares*) as a function of volume fraction Φ_m taken from the shear ramp experiment

The two fits (solid and dashed lines) meet at lower volume fractions (at $\Phi_m \approx 0.03$), which might be an additional reason, why accurate determination of $\dot{\gamma}_c$ was not possible at the lowest membrane volume fraction. The respective data point is therefore omitted from the presentation.

Again the existence of a two-phase region between L_3 and L_α (shear-induced) indicates the first-order nature of the transition. As mentioned earlier, the birefringence of the shear-induced L_α-phase is zero due to its parallel orientation in the shear field. The two-phase region between L_α and L_3, in addition to increased turbidity, displays birefringence (Fig. 2). This can be attributed either to the presence of deformed droplets of L_α-phase that consequently display birefringence or to a perpendicular orientation of lamellae in the shear field. The latter has already been observed in similar systems and was also predicted by theory [5, 23].

Shear-rate quench

In a last set of experiments we studied the relaxation of the shear aligned L_α-phase back to the isotropic state by performing a shear quench using birefringence and transmission to trace the transition. The quench was performed from a shear rate about 30% higher than $\dot{\gamma}_c$ to 10 s^{-1} and hence the relaxation in all cases started from the fully shear-aligned state. Only for the lowest volume fraction was the sample quenched to 0.4 s^{-1}.

Transmission and birefringence initially drop abruptly upon reducing the shear rate to 10 s^{-1}. This might be because of a disturbance of the homeotropic alignment of bilayers upon stopping shear.

Eventually a fully isotropic distribution of bilayers will be reached and consequently the birefringence converges to zero. This relaxation of the signals seems to obey an exponential form (Fig. 7). A time $t = 0$ was defined at the minimum of the transmission and birefringence signals, respectively. Note that the nucleation of the L_3-phase is not considered by omitting the first part of the signal, because data evaluation starts in the two phase region and thus the L_3-phase has already nucleated. The underlying process for the relaxation of birefringence and transmission might be the formation of handles.

The results of one relaxation experiment with a sample of $\Phi_m = 0.1163$ are shown in Fig. 7 along with best fits from an exponential (transmission) and a biexponential decay (birefringence). The relaxation times τ_{slow} from transmission and birefringence are very similar, whereas τ_{fast} from birefringence is about one order of magnitude smaller. The results for all volume fractions are summarized in Fig. 8 and compared with the inverse of the critical shear rate from shear ramp experiments, which should correspond to the topological relaxation time of the system.

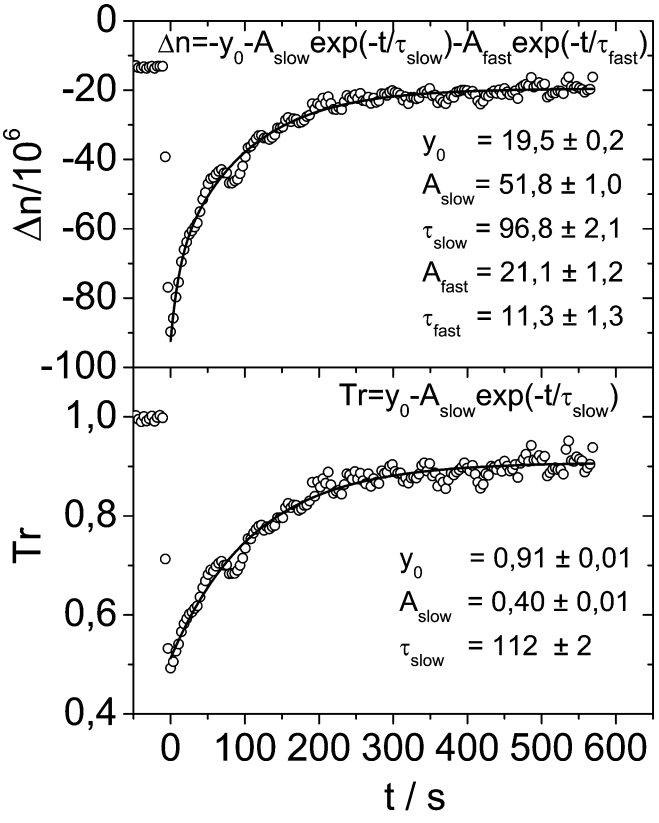

Fig. 7 Measurement of the characteristic relaxation time studied by a shear rate quench from $\dot{\gamma}_c$ to $\gamma = 10\ s^{-1}$. Here $\Phi_m = 0.1163$ and $T = 42$ °C, and the quench was performed from 350 s^{-1}. *Lines* represent exponential and biexponential fits to the transmission and the birefringence, respectively

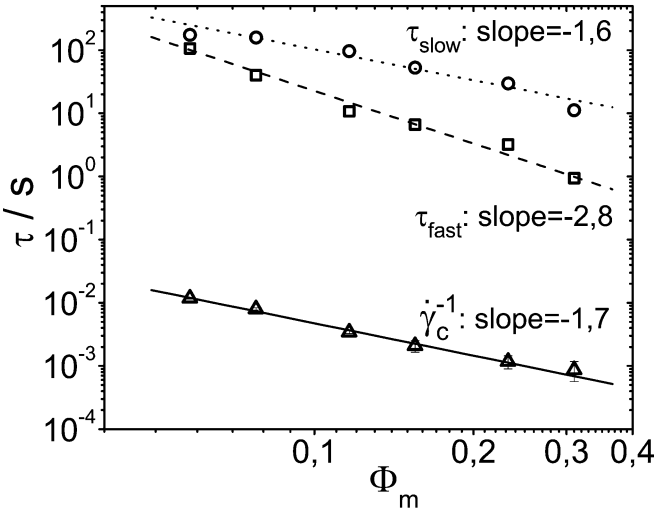

Fig. 8 Comparison of the relaxation times obtained from the different experiments. τ_{slow} and τ_{fast} are the relaxation times obtained from fitting a biexponential function to the birefringence data of the relaxation experiment. The inverse of the critical shear rate obtained from shear ramp experiments is compared with the above mentioned relaxation times

The inverse critical shear rate is identical with neither τ_{slow} nor τ_{fast}. One reason is the nature of the experiment. The detection of relaxation times of the order of microseconds or milliseconds is impossible in a relaxation experiment performed as it was here. This would, however, be necessary if one wanted to observe the relaxation of the bilayer fluctuations, which were suppressed by shear. It is, nevertheless, interesting that a relaxation is observed on longer time scales, which in addition has a similar scaling with membrane volume fraction. Thus the relaxation back to the isotropic state has a different time constant. Bearing in mind that the shear alignment is a process in the presence of a field, whereas the relaxation to the isotropic state is almost field-free, this asymmetry is not necessarily contradictory. On the other hand, processes on larger length scales, where rearrangement of domains of bilayer material might be involved, lead to different magnitudes of the relaxation times and inverse critical shear rates. Interestingly, at low membrane volume fractions the values found in *T*-jump experiments using the same system are of similar magnitude to the relaxation times observed in the shear quench experiments, although they display different scaling behavior [23].

Because the birefringence revealed two relaxation times, there have to be two processes involved. One mechanism might be a local process involving the formation of handles and the relaxation of the distorted lattice, which is a necessary consequence of the transition from a one- to a three-dimensional arrangement of bilayers. This is associated with a change of the lattice constant, i.e. the correlation length ξ of the L_3-phase, which is about 1.5 times the lamellar spacing of the L_α-phase with the same membrane volume fraction. Thus an intermediate state could be a distorted L_3-phase, which relaxes to the fully isotropic L_3-phase. The other might be shape relaxation of the initially deformed L_3-domains. Both contributions lead to a decrease in the birefringence signal. The fast relaxation most probably comprises the rearrangement of bilayer material and relaxation of the distorted lattice, whereas the slow relaxation is probably connected to the growth of the L_3-domains.

Also, the evolution of transmission displays a single relaxation time very similar to τ_{slow}, indicating again that the slow relaxation time might be associated with the growth of L_3-domains. These two mechanisms, rearrangement of bilayer material, and growth of the L_3-domains, might explain the biexponential behavior of the relaxation process as it is observed in the birefringence. The growth of the L_3-domains is probably associated with a shape relaxation of initially deformed L_3-droplets.

A video sequence of such a shear quench experiment is added as supporting information to illustrate this relaxation process. The video displays the process for a sample with $\Phi_m = 0.31$. As one can see, the turbidity in the center of the shear geometry vanishes quickly upon the shear rate quench. However, the initial drop in transmission, as it is observed in the shear quench experiments (Fig. 7), cannot be observed visually, because it is not sufficiently pronounced to be resolved by the naked eye.

Discussion

Three types of experiment were conducted to study the influence of shear on the L_3-phase, namely temperature-dependence experiments at different constant shear rates, isothermal shear ramps, and shear quench experiments. The Φ_m-dependence of the critical shear rate reveals discrepancies to current theories. The origin of this discrepancy is, however, not yet fully understood. It could very well be a dependence of the viscosity on membrane volume fraction that alters the general scaling predicted by Eq. (1).

The shear quench experiments on the other hand, yielded interesting information about the relaxation back to the undisturbed, isotropic state. Careful control of the starting conditions, however, was necessary. This experiment can be compared with the temperature-jump experiments, in which a relaxation from a perturbation back to the isotropic state is also observed. As already mentioned, the relaxation times at low Φ_m are of comparable magnitude, but the overall scaling is different. In both cases the underlying process leading to the relaxation is the formation of handles and hence similar scaling should be observed. Yet the starting conditions are different, i.e., here we start from a well aligned anisotropic state and Le et al. started from the L_3–water coexistence. In this respect it would be interesting to study the Φ_m-dependence of the relaxation times in temperature-jump experiments starting from the L_α-phase.

Relaxation experiments similar to those presented here were also performed by Mahjoub et al. [10]. They however, found a dependence of relaxation times on shear rate and shearing time, i.e. shear history effects. These influences were not found in the study presented here, because care was taken to guarantee identical starting conditions for the different relaxation experiments.

The relaxation times found in the shear quench experiments differ by orders of magnitude from the inverse critical shear rate. It is most probable that other processes are involved on different length scales, i.e. the topological relaxation involved in the relaxation of the shear aligned back to the isotropic state is much slower than the bilayer fluctuations, which are suppressed by shear. At least for τ_{fast} the general Φ_m^3-scaling applies and the scale invariance argument seemingly holds for

these processes also, which as such is a striking observation.

The L_3-phase is a very delicate system for experimentalists, owing to its narrow concentration and temperature range in the phase diagram of nonionic surfactants. Especially problematic is the selective evaporation of components. This has on some occasions proved to be the reason for unreasonably low critical shear rates [11, 12]. In our experiments, however, the component with the lowest vapor pressure is water (32 mbar at 25 °C and 73 mbar at 40 °C [24]). The boiling point of *n*-decane is 174 °C and its vapor pressure at 25 °C is 1.7 mbar. Thus the only condition that can change in our system during the experiment is the membrane volume fraction, not the membrane thickness. This would, however, lead to a higher critical shear rate than expected and thus is contrary to our findings. We are confident that the sample composition was constant during one experiment and that there were no temperature gradients within the sample (see Experimental section).

There is a fundamental difference of our system from that studied by Porcar et al. Our system is constituted of a swollen bilayer and as such it is more complex. The system studied by Porcar et al. was a pure surfactant/water L_3-phase whereas in our work the swollen bilayer might imply a more complex velocity gradient profile across the bilayer. It is possible that the general scale invariance argument of Porte et al. [25] for L_3-phases that leads to the Φ^3-scaling of the free energy per unit volume is still applicable, but the solvent viscosity needs to be replaced by that of the sample, which itself depends on membrane volume fraction and therefore would lead to a different scaling of $\dot{\gamma}_c$.

Again, we want to point out the difference of our experiments to the *T*-jump experiments performed by Le et al. on the same system [17, 18, 19]. The *T*-jump is performed starting from the L_3-phase, heating into the L_3 + water two-phase region. Then relaxation of the disturbed L_3-phase back to its equilibrium state is observed. Increasing the shear rate in our experiments yields a L_α-phase and relaxation in the shear quench experiments is observed from this shear-aligned state back to the isotropic phase. This might explain the different scaling with Φ_m as found in the two studies.

The scaling of the critical shear rate with Φ_m found here resembles the Φ_m^2-dependence of the phase boundaries at rest [18]. We thus suggest that in our case the transition from the L_3- to the shear aligned L_α-phase should be discussed in terms of an underlying first-order phase transition, as is also found for wormlike micelles [6, 7, 8].

Conclusions

In conclusion, this study showed that the L_3-to-lamellar transition under shear can be examined by rheo-birefringence. This study revealed weaker Φ_m-dependence of the critical shear rate than expected from theory (Eq. 1) or in comparison with experiments performed by Porcar et al. However, it has been argued that the viscosity in Eq. (1) should be the sample viscosity, which itself is Φ_m-dependent, and smaller power-law exponents for the critical shear rate were found in other studies also [10]. Furthermore, the relaxation experiments from the shear-aligned state back to the isotropic, were possible by careful control of the starting conditions.

Interestingly, the relaxation from the shear-aligned back to the isotropic state displayed different scaling with membrane volume fraction than that studied in temperature-jump experiments. Although the process leading to the relaxation, namely the topological relaxation by formation of handles, is probably identical in both cases, the starting conditions are different. This might explain the different findings.

Acknowledgments We thank the Deutsche Forschungsgemeinschaft, the Fond der Chemischen Industrie and the Swedish Science Council (VR) for financial support.

References

1. Butler P (1999) Curr Opin Colloid Interface Sci 4:214
2. Richtering W (2001) Curr Opin Colloid Interface Sci 6:446
3. Diat O, Roux D (1995) Langmuir 11:1392
4. Cates ME, Milner ST (1989) Phys Rev Lett 62:1856
5. Bruinsma R, Rabin Y (1992) Phys Rev A 45:994
6. Porte G (1996) Curr Opin in Colloid Interface Sci 1:345
7. Porte G, Appell J, Bassereau P, Marignan M, Skouri M, Billard I, Delsanti M, Candau SJ, Strey R et al (1991) Prog Colloid Polym Sci 84:264
8. Porte G, Appell J, Bassereau P, Marignan J (1989) J Phys 50:1335
9. Porte G, Berret J-F, Harden JL (1997) J Phys II 7:459
10. Mahjoub HF, McGrath KM, Kleman M (1996) Langmuir 12:3131
11. Mahjoub HF, Bourgaux C, Sergot P, Kleman M (1998) Phys Rev Lett 81:2076
12. Butler PD, Porcar L, Hamilton WA, Warr GG (2002) Phys Rev Lett 88:9601
13. Porcar L, Hamilton WA, Butler PD, Warr GG (2002) Phys Rev Lett 89:8301

14. Strey R, Schomäcker R, Roux D, Nallet F, Olsson U (1990) J Chem Soc Faraday Trans 86:2253
15. Strey R, Winkler J, Magid L (1991) J Phys Chem 95:7502
16. Lei N, Safinya CR, Roux D, Liang KS (1997) Phys Rev E 56:608
17. Le TD, Olsson U, Wennerström H, Uhrmeister P, Rathke B, Strey R (2002) J Phys Chem B 106(36):9410
18. Le TD, Olsson U, Wennerström H, Schurtenberger P (1999) Phys Rev E 60:4300
19. Schwarz B, Moench G, Ilgenfritz G, Strey R (2000) Langmuir 16:8643
20. Waton G, Porte G (1993) J Phys II 3:515
21. Yamamoto J, Tanaka H (1996) Phys Rev Lett 77:4390
22. Larson RG (1992) Rheol Acta 31:497
23. Le TD, Olsson U, Mortensen K (2001) Phys Chem Chem Phys 3:1310
24. West RC, Astle MJ, Beyer WH (1986–1987) (eds) CRC Handbook of Chemistry and Physics, 67th edn
25. Porte G, Delsanti M, Billard I, Skouri M, Appell J, Marignan J, Debeauvais F (1991) J Phys II 1:1101